Optica Applicata, Vol. XXXIX, No. 1, 2009

All-optical frequency down-conversion based on cross-phase modulation in high nonlinearity dispersion-shifted fiber for WDM radio over fiber application

HONGWU YANG, JUNQIANG SUN*, QIUJIAO DU

Wuhan National Laboratory for Optoelectronics, School of Optoelectronic Science and Engineering, Huazhong University of Science and Technology, Wuhan 430074, Hubei, P.R. China

*Corresponding author: jqsun@mail.hust.edu.cn

Simultaneous all-optical frequency down-conversion technique based on cross-phase modulation in a high nonlinearity dispersion-shifted fiber is proposed and verified by simulation, and its application to a wavelength-division-multiplexing (WDM) radio over fiber (ROF) is proposed. Error-free simultaneous all-optical frequency down-conversion of the 16 WDM ROF upstream channels is achieved. The simulated results show the performance of WDM signals is in good accordance with a single signal without any interference, and the power difference of two beat frequencies of the down-conversion signal is independent of the optical local oscillator power. The wavelength span of larger than 20 nm for down-conversion signal can be obtained.

Keywords: all-optical frequency down-conversion, radio over fiber (ROF), wavelength division multiplexing (WDM), cross-phase modulation (XPM), modulation instability, high nonlinearity dispersion-shifted fiber (HNL-DSF).

1. Introduction

The application of radio over fiber (ROF) for broad-band wireless access system having a high data rate at a millimeter wave frequency band becomes more prevalent because it can offer broad-band radio access to a large number of customers. For a reduction in the total cost of the ROF system and the complexity of the architecture, satisfying more end-users between central and base stations at the same time, a solution to seamlessly integrate the wavelength-division-multiplexing (WDM) or WDM passive optical network transport systems with ROF access system to take full advantage of its ultra-wide bandwidth characteristics is desirable. Numerous remote antenna stations need to be simplified, and the central station becomes complicated including a data modulation/demodulation and up/down-conversion. For a successful implementation of WDM ROF systems, all-optical conversion for WDM signals is

the key issue to be solved [1–3]. The techniques, based on the four-wave mixing (FWM) effect in a nonlinear fiber or waveguide device, have low conversion efficiency and need very high input optical power [4]. The other all-optical conversion technique is based on cross-gain modulation or cross-phase modulation (XPM) in semiconductor optical amplifiers (SOA) [5, 6]. But these SOA-based methods are difficult to mix data signals with high-frequency local oscillator signals efficiently owing to narrow modulation bandwidth of the SOA [7]. Furthermore, another major hurdle is the inherent carrier saturation effect in SOA [8], which results in the reduction of the WDM channel number and greatly limits the quantity of wireless end users. In this paper, an all-optical frequency down-conversion technique utilizing a HNL-DSF in a WDM-based ROF uplink system is proposed. The proposed down-conversion scheme shows features including broad bandwidth, capability of simpler configuration, simultaneous conversion, and high conversion efficiency. In addition, an error-free simultaneous down--conversion of 16 WDM ROF upstream channels that carry 2.5 Gb/s amplitude shift keying (ASK) data at 44 GHz to an optical intermediate frequency (IF) signal at the frequency of 4 GHz is verified by simulating with the software of OptiSystem 3.1. The results show that this scheme exhibits very good conversion performance at a high data rate and can provide more wavelength channels by being extended into the whole optical fiber transmission band without any interference and carrier saturation effect limitation.

2. Theory and simulation analysis

When a signal at wavelength lying in the normal group velocity dispersion (GVD) propagates together with the other signal at wavelength lying in the anomalous GVD, modulation instability can be induced owing to the cross-phase modulation. In the conditions, if strong pump light is in the form of a pulse and the other is a weak continuous-wave (CW) light in the anomalous GVD, modulation instability can induce the generation of pulse from the CW signal [9]. The main differences between ref. [9] and our proposed idea are that the CW light is replaced by a weak pulse signal with 44 GHz repetition frequency and the conclusion is applied to ROF system. The other difference is that pump light lies in different dispersion region. According to ref. [10], we know that XPM induced modulation instability can occur in a conventional fiber when one of the light waves propagates in the anomalous-dispersion regime. When pump light lies in the spectral region of anomalous dispersion, modulation instability can also occur whether the CW light frequency is in the normal- or anomalous--dispersion regime. As a result, CW light gradually evolves into pulse and the repetition frequency of the converted pulse is equal to the modulation frequency of the pump pulse. Furthermore, modulation instability is suppressed by the presence of a large difference between the pump light and signal light group velocities. To minimize the group velocity mismatch, an extremely short high nonlinear fiber in contrast to conventional fiber is used and the wavelength of a signal pulse and a pump pulse should roughly correspond to two opposite sides of the dispersion curve of a used fiber.

The propagation of the RF pulse, co-propagating local oscillator (LO) pulse in HNL-DSF can be expressed by the following coupled nonlinear Schrödinger equations [11]:

– RF pulse

$$\frac{\partial A_1}{\partial z} + \frac{1}{v_1}\frac{\partial A_1}{\partial t} + \frac{i}{2}\beta(\lambda_1)\frac{\partial^2 A_1}{\partial t^2} + \frac{1}{2}\alpha A_1 = i\gamma_1\left[|A_1|^2 + 2|A_2|^2\right]A_1 \qquad (1)$$

– LO pulse

$$\frac{\partial A_2}{\partial z} + \frac{1}{v_2}\frac{\partial A_2}{\partial t} + \frac{i}{2}\beta(\lambda_2)\frac{\partial^2 A_2}{\partial t^2} + \frac{1}{2}\alpha A_2 = i\gamma_2\left[|A_2|^2 + 2|A_1|^2\right]A_2 \qquad (2)$$

Here λ_i (i = 1, 2) is the wavelength, A_i (i = 1, 2) is the propagating optical field amplitude, v_i is the group velocity, $\beta(\lambda_i)$ is the linear group velocity dispersion given by $-(\lambda_i^2 D_i / 2\pi c)$, where D_i is the dispersion parameter, c is the speed of light, the nonlinear coefficient γ_i is 20 km^{-1}W^{-1}; α is the loss of the HNL-DSF, and we assume that it is independent of wavelength (α = 0.25 dB/km). GVD, self-phase modulation, and XPM are taken into account in our model. In our simulations, the full-width at half-maximum (FWHM) pulse width, center wavelength λ_{RF}, repetition frequency and peak power of RF pulse are 10 ps, 1552 nm, 44 GHz and 0 dBm, respectively. The center wavelength λ_{LO}, peak power, repetition frequency and FWHM pulse width of control pulse are 1558 nm, 22 dBm, 40 GHz, and 10 ps, respectively. The length of the HNL-DSF is 200 m. It is a HNL-DSF with zero-

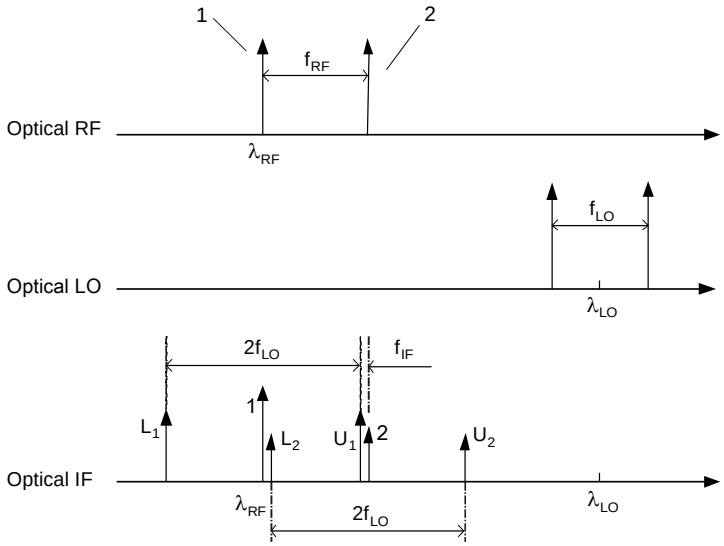

Fig. 1. Conceptual diagram of frequency conversion.

-dispersion wavelength of 1550.7 nm, dispersion slope of 0.03 ps/nm^2/km and effective fiber core area of 11 μm^2.

Figure 1 shows conceptual diagrams of numerical simulation. Both frequency components of the RF pulse generate two 40 GHz sidebands respectively. It is similar to the double sideband modulation by using a Mach–Zehnder electro-optic modulator. As a result, the frequency down-conversion from f_{RF} to $f_{IF} = f_{RF} - f_{LO}$ can be achieved by beating frequency components 2 and U_1. Numerical simulations are performed using the difference approach. The simulation results are shown in Fig. 2. The origin of the x-coordinate represents the carrier wavelength λ_{RF} and there is a sideband at 40 GHz shown clearly, which is the sideband U_1 of the frequency component 1 of the RF pulse. And also at the 84 GHz, the sideband U_2 of the frequency component 2 of the RF pulse can be seen clearly.

To achieve f_{IF}, frequency components 2 and U_1 must be coherent. Figure 3 shows phase shift of the converted RF signal. Because frequency components 1 and 2 are coherent, we study component 1 and U_1. The Table shows phase difference of

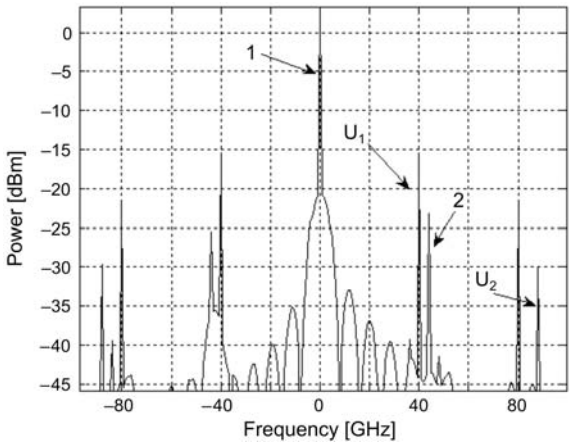

Fig. 2. Results of numerical simulation.

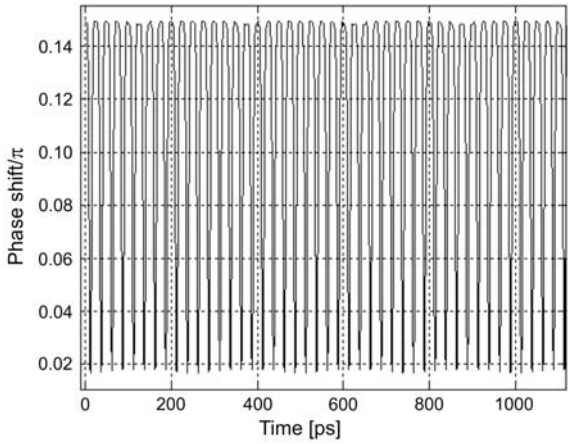

Fig. 3. Phase shift of the converted RF signal.

T a b l e. The phase shift of frequency components 1 and U_1.

Fiber length [m]	Phase difference of frequency components 1 and U_1 [dB]	Difference value [dB]
200	–50.5—(–56.4)	5.9
300	–48.7—(–54.6)	5.9
400	–47.5—(–53.4)	5.9
500	–46.5—(–52.4)	5.9
600	–45.7—(–51.6)	5.9

frequency components 1 and U_1 at different fiber length. Difference values are constant, which indicate that frequency components 1 and U_1 are coherent. So, component 2 and U_1 are coherent, f_{IF} can be achieved by beating frequency components 2 and U_1.

3. Concept of all-optical frequency down-conversion

Figure 4 shows conceptual diagrams of experiment setup. As can be seen in Fig. 4**a**, the optical RF signal that is intensity modulated at the RF band (f_{RF}) and the optical LO signal that is intensity modulated at the frequency of f_{LO} are coupled to the HNL-DSF. An optical IF signals containing a harmonic component of $f_{\mathrm{RF}}-2f_{\mathrm{LO}}$

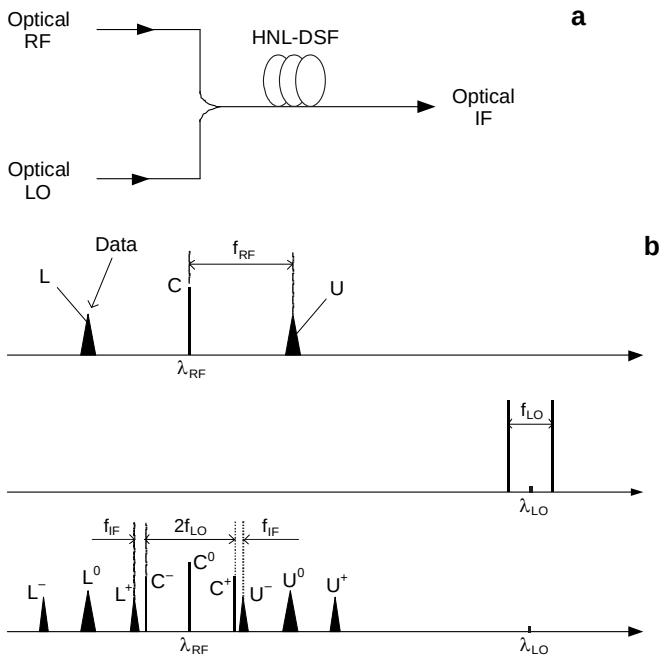

Fig. 4. Conceptual diagram of all-optical frequency down-conversion system (**a**). Optical spectra of the RF, LO, and IF signals (**b**).

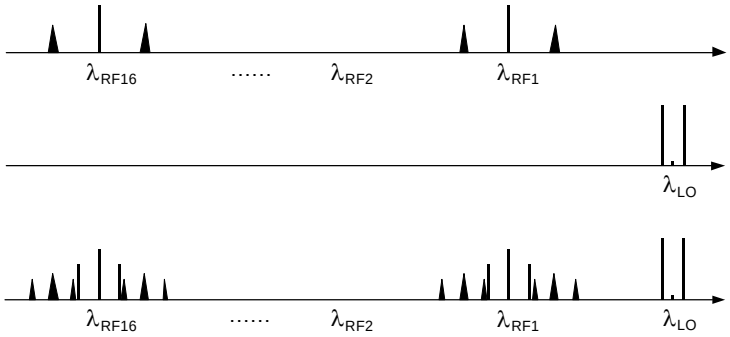

Fig. 5. Optical spectra of the RF, LO, and IF signals with simultaneous all-optical frequency down--conversion.

can be generated at the output port of the HNL-DSF. The operational principle of the all-optical down-conversion can be explained in the wavelength domain. Figure 4**b** shows the optical spectra of the optical RF, LO, and IF signals. The optical RF signal is assumed to be in a double sideband format. Three components (the carrier and the first sidebands) in the optical spectra are considered. The *U*, *L*, and *C* represent the upper sideband, the lower sideband, and the optical carrier components, and the superscripts of "–" and "+" represent the optical frequency shift to the higher ($\Delta f = +f_{LO}$) and the lower ($\Delta f = -f_{LO}$) frequency directions, respectively. At the output port, frequency-shifted signal components (L^+, C^+, U^+, and L^-, C^-, U^-) are generated due to the modulation instability in the HNL-DSF. Now a desired down-converted signal component (f_{IF}) is obtained through an optical heterodyne detection by using a photodetector if the frequency components involved in beat frequencies L^+ and C^- or C^+ and U^- are coherent. Because (C, L, U) is coherent [12], according to simulation results above, (C^+, U^-) or (C^-, U^+) is coherent. As a result, the frequency down--conversion from f_{RF} to $f_{IF} = f_{RF} - 2f_{LO}$ can be achieved. In addition, the carried wavelength of the down-converted IF signal is identical to that of the input optical RF signal (λ_{RF}). Thus, several wavelength multiplexed RF signals can be simultaneously down-converted using a single HNL-DSF, which can reduce the number of components and the complexity of the ROF system.

Figure 5 shows the optical spectra with simultaneous all-optical down-conversion approach. As shown in Fig. 5, an upstream data signal centered at f_{RF} is E/O converted to a WDM optical RF signal having a wavelength of λ_{RFi} (where i is the channel index). Optical RF signals are multiplexed and input to the HNL-DSF for a simultaneous down-conversion with the optical LO signal having the wavelength of λ_{LO}. The down--converted optical IF signals ($\lambda_{IFi} = \lambda_{RFi}$) having the frequency of $f_{IF} = f_{RF} - 2f_{LO}$ are detected by a receiver in the central station (CS) assigned to each channel. Because there are sixteen RF optical channels, GVD induced walk-off between LO pulse and signal pulse should be decreased by using a HNL-DSF with zero dispersion wavelength of 1550.7 nm and total dispersion and relative group delay are shown in Fig. 1 from ref. [13]. Sixteen weak signal pulses at different wavelengths are propagated in a fiber

with a strong LO pulse. The wavelength of signal light is chosen to be from 1533 to 1558 nm and the LO light wavelength is 1564 nm. This proposed system using the single HNL-DSF has advantages making the WDM ROF system simple. The frequency down-conversion is achieved in the optical domain in which, if the frequency of the signals to be processed in CS is low. Accordingly, no expensive components including high speed photodetectors, amplifiers, and frequency mixers operating at a high frequency are required in the CS.

4. Numerical verification

To verify the validity of our proposed approach, a ROF system with our proposed all-optical frequency down-conversion technique is simulated, as shown in Fig. 6.

Parameters of the HNL-DSF are chosen to be 1550.7 nm at zero dispersion wavelength, 200 m long and 20 $km^{-1}W^{-1}$ of nonlinear coefficient. In order to generate sixteen neighboring WDM ROF upstream channels (optical RF signals), sixteen DFB laser diodes having wavelengths from 1533.925 to 1557.838 nm with adjacent 200 GHz spacing are employed. Output powers are set to be equal. The electrical RF signal is generated by the electrical frequency up-conversion of a 2.5 Gb/s ASK

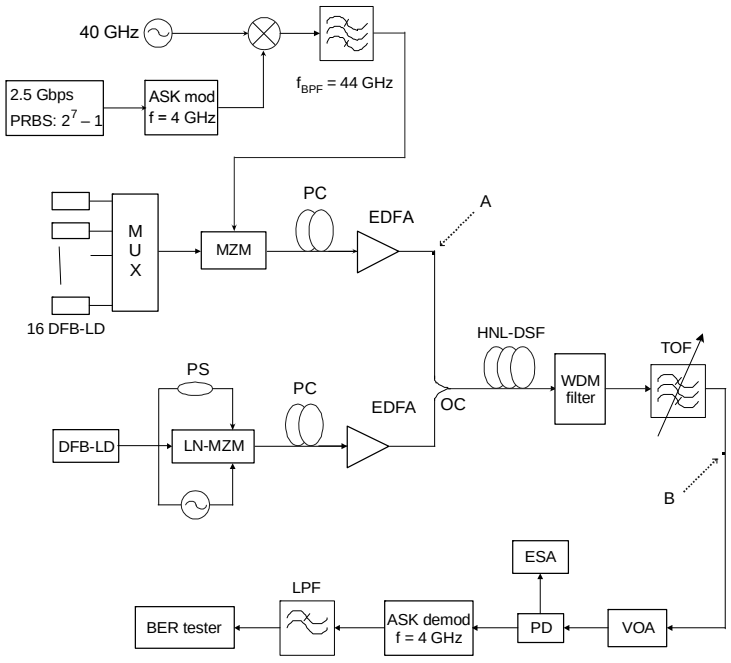

Fig. 6. Simulative setup for simultaneous down-conversion. EDFA: Er-doped fiber amplifier; LN-MZM: $LiNbO_3$ Mach–Zehnder modulator; PS: phase shifter; TOF: tunable optical filter; PD: photodiode; VOA: variable optical attenuator; PRBS: pseudorandom bit sequence; ESA: electrical spectrum analyzer; DFB-LD: distributed feedback laser diode; LPF: low pass filter; OC: optical coupler; ASK mod: amplitude shift keying modulator; ASK demod: amplitude shift keying demodulator.

signal at 4 GHz with a 40 GHz LO source. The optical power of the 44 GHz optical RF signals (f_{RF}) fixes at approximately 0 dBm per channel by erbium-doped fiber amplifier (EDFA). The 20 GHz LO signal at a wavelength of 1564 nm is used as the pump signal, which is generated by driving a $LiNbO_3$ Mach–Zehnder modulator biased at V_π with two complementary 10 GHz sinusoid waveforms. The modulation frequency of the generated LO optical signal is 20 GHz and the LO signal is amplified via an EDFA. The generated sixteen multiplexed optical RF signals and modulated by the optical LO signal are coupled to the HNL-DSF subsequently. And then they are converted to an IF signal by a photodetector. The electrical powers of the down--converted signal ($f_{IF} = f_{RF} - 2f_{LO}$) are measured by using an electrical spectrum analyzer.

Figures 7 and 8 show the optical spectra of the optical RF and the optical IF signal, respectively, when the λ_{RF} is 1557.838 nm. As can be seen in Fig. 7, the intensity

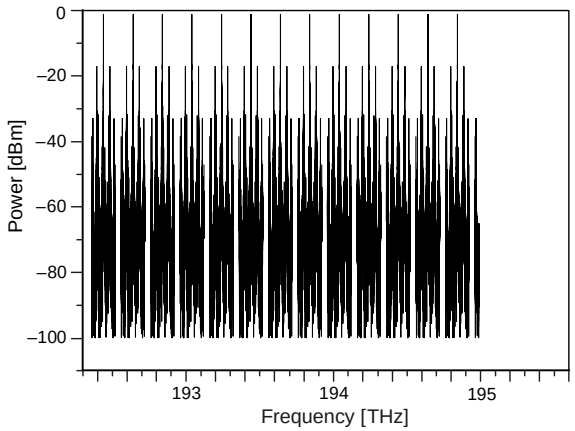

Fig. 7. Optical spectra of RF signal at the DWDM multiplexer output (at the position A of Fig. 6).

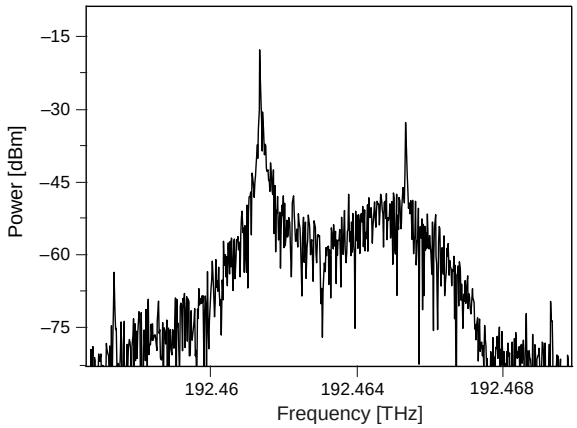

Fig. 8. Optical spectrum of a filtered down-converted signal at wavelength 1557.838 nm (at the position B of Fig. 6).

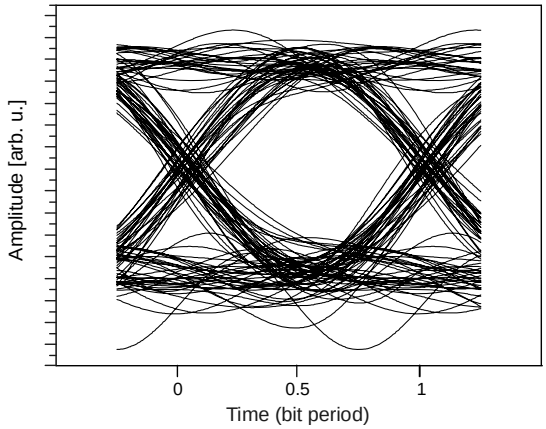

Fig. 9. Eye diagram for recovered 2.5 Gb/s signal from the down-converted signal at 1557.838 nm.

difference between the first and the second sideband is approximately 16 dBm, and the higher order sideband components can be neglected. Upper and lower shifted components, which may include the frequency-shifted carrier and data signal (C^-/L^+ and C^+/U^-, respectively, shown in Fig. 4), are clearly observed. Uniform conversion characteristics of the sixteen WDM ROF upstream channels are similar to those of the single upstream channel. The converted signals are separated from the LO signal by using a WDM filter and a tunable optical filter with a bandwidth of 4 GHz is used to realize single wavelength filtering. Then frequency components 2 and U_1 are filtered and a down-converted signal is obtained by optical electrical conversion via a PIN photodiode. The power control is conducted by the variable optical attenuator. The measured eye diagram after down-conversion at a wavelength of 1557.838 nm is shown in Fig. 9 when the LO power is 22 dBm. A wide open and clean eye diagram is obtained from BER analyzer.

The receiver sensitivity of all 16 down-converted channels is measured via tuning a tunable optical filter. It is shown in Fig. 10 as a square symbol. We can see that

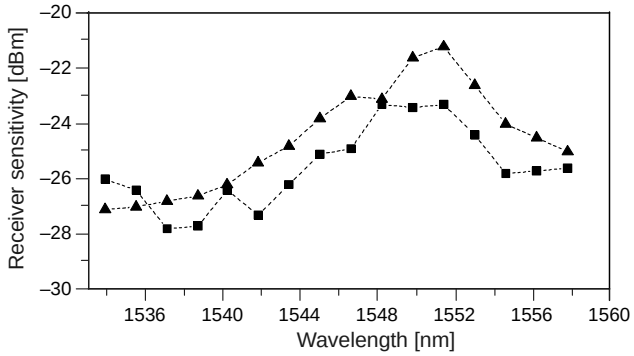

Fig. 10. Receiver sensitivity of 16 down-converted signals; ▲ – down-conversion of a single channel, ■ – simultaneous down-conversion of 16 channels.

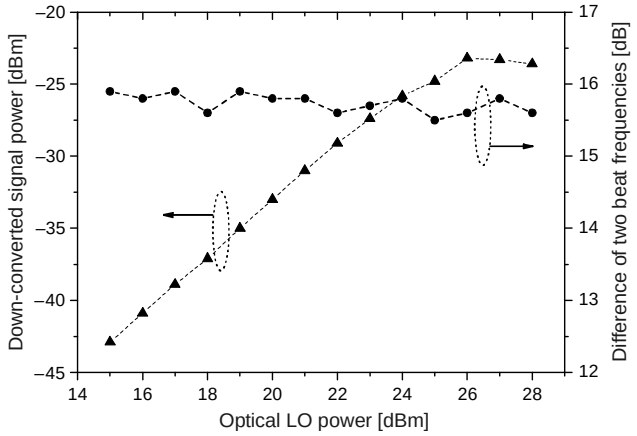

Fig. 11. Optical power of the down-conversion signal and power difference of the two beat frequencies as a function of input LO signal power.

the receiver sensitivity at 10^{-9} of all 16×2.5 Gb/s wavelengths is between –22 dBm and –28 dBm, and the maximum difference among them is less than 5 dB. The difference of power for down-converted signals conforms to the corresponding difference of the differential group delay between the LO pulse and signal pulse. To investigate the multi-channel interference in a HNL-DSF, the DFB laser array source is replaced with a tunable laser source whose range covers the whole *C*-band while keeping the LO power (22 dBm) the same as the total power of 16 wavelength channels. Sixteen wavelengths are measured respectively, which is also shown in Fig. 10 as a triangle symbol. The maximum difference of receiver sensitivity at 10^{-9} is observed nearby the zero dispersion wavelength. The difference among most of them is within 2 dBm and the multi-channel propagation increases the receiver sensitivity nearby zero dispersion wavelength.

In Figure 11, we observe that below 28 dBm, the difference of the beat frequencies C^+ and L^- almost does not change. But the sideband signal power reduces monotonously following the decrease of the optical LO power because of the weak XPM, which leads to a great degradation of optical signal-to-noise ratio for the down-converted signal. The actual information is transmitted in the sideband, so a stable C^+ to L^- difference will lead to satisfying receiver sensitivity. The maximum optical RF power is mainly limited by the power level for FWM, where the FWM and inter-channel crosstalk are induced. Too large control signal power results in extra nonlinear effects such as FWM, stimulated Brillouin scattering, and stimulated Raman scattering. The range of the optical LO power is between 15 and 28 dBm, and the value of 22 dBm is chosen in order to investigate the system performance at a low signal-to-noise ratio condition.

We choose four wavelengths at 1535.497 nm, 1541.814 nm, 1546.587 nm and 1556.221 nm, respectively, which are shown in Fig. 12. It can be seen that the optimum length of the HNL-DSF is between 200 and 300 m. Below 200 m, the receiver sensitivity at 10^{-9} degrades too quickly because of the weak XPM. For the channels

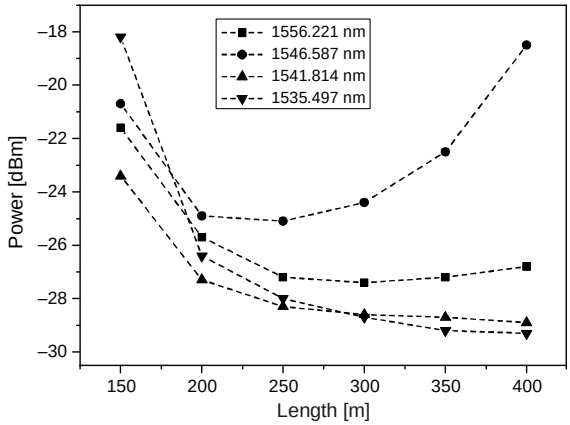

Fig. 12. Receiver sensitivity as a function of the HNL-DSF length.

near the zero dispersion wavelength, increasing the length will induce a large walk-off between the LO pulse and signal pulse, and consequently reduce the receiver sensitivity. It is stressed that the simulation is only performed with the 200 m HNL-DSF and that optimizing fiber parameters such as dispersion, nonlinearity and length will clearly improve the conversion efficiency and the receiver sensitivity.

5. Conclusions

We have verified by simulation that sixteen WDM optical RF signals that carry 2.5 Gb/s ASK data at 44 GHz are well simultaneously down-converted to 4 GHz based on XPM in a HNL-DSF. All 16 wavelengths show almost identical performance. A proper LO power is between 21 and 26 dBm. Too large LO power will result in extra nonlinear effects. Our simulated results show that the influence of the LO power on the beat frequency power difference of the down-conversion signal can be ignored and the optimum length of the HNL-DSF is between 200 and 300 m. Results indicate that the scheme has very good conversion performance at a very high data rate and can provide a very useful solution for more wavelength channel applications at all bands without any interference and saturation limitation in ROF systems.

References

[1] SEO Y.K., SEO J.-H., CHOI W.-Y., *Photonic frequency-upconversion efficiencies in semiconductor optical amplifiers*, IEEE Photonics Technology Letters **15**(5), 2003, pp. 751–753.

[2] YU J., GU J., LIU X., JIA Z., CHANG G.-K., *Seamless integration of an 8 2.5 Gb/s WDM-PON and radio-over-fiber using all-optical up-conversion based on Raman-assisted FWM*, IEEE Photonics Technology Letters **17**(9), 2005, pp. 1986–1988.

[3] SHIN D.S., LI G.L., SUN C.K., PAPPERT S.A., LOI K.K., CHANG W.S.C., YU P.K.L., *Optoelectronic RF signal mixing using an electroabsorption waveguide as an integrated photodetector/mixer*, IEEE Photonics Technology Letters **12**(2), 2000, pp. 193–195.

[4] LEESTI B., ZILKIE A.J., AITCHISON J.S., MOJAHEDI M., WANG R.H., ROTTER T.J., YANG C., STINTZ A., MALLOY K.J., *Broad-band wavelength up-conversion of picosecond pulses via four-wave mixing in a quantum-dash waveguide*, IEEE Photonics Technology Letters **17**(5), 2005, pp. 1046–1048.

[5] SEO J.-H., SEO Y.-K., CHOI W.-Y., *Nonlinear characteristics of an SOA photonic frequency up-converter*, [In] *MWP 2003 Proceedings. International Topical Meeting on Microwave Photonics*, 2003, pp. 109–112.

[6] SONG H.-J., LEE J.-S., SONG J.-I., *Signal up-conversion by using a cross-phase-modulation in all-optical SOA-MZI wavelength converter*, IEEE Photonics Technology Letters **16**(2), 2004, pp. 593–595.

[7] YU J., JIA Z., CHANG G.-K., *All-optical mixer based on cross-absorption modulation in electroabsorption modulator*, IEEE Photonics Technology Letters **17**(11), 2005, pp. 2421–2423.

[8] SONG H.-J., LEE J.-S., SONG J.-I., *All-optical harmonic frequency up-conversion for a WDM radio over fiber system*, [In] *2004 IEEE MTT-S International Microwave Symposium Digest*, Vol. 1, 2004, pp. 405–407.

[9] SCHADT D., JASKORZYNSKA B., *Generation of short pulses from CW light by influence of crossphase modulation (CPM) in optical fibers*, Electronics Letters **23**(20), 1987, pp. 1090–1091.

[10] YU M., MCKINSTRIE C.J., AGRAWAL G.P., *Instability due to cross-phase modulation in the normal--dispersion regime*, Physical Review E **48**(3), 1993, pp. 2178–2186.

[11] AGRAWAL G.P., *Nonlinear Fiber Optics*, Academic Press, New York 1999.

[12] O'REILLY J.J., LANE P.M., HEIDEMANN R., HOFSTETTER R., *Optical generation of very narrow linewidth millimetre wave signals*, Electronics Letters **28**(25), 1992, pp. 2309–2311.

[13] YU J., ZHENG X., PEUCHERET C., CLAUSEN A.T., POULSEN H.N., JEPPESEN P., *All-optical wavelength conversion of short pulses and NRZ signals based on a nonlinear optical loop mirror*, Journal of Lightwave Technology **18**(7), 2000, pp. 1007–1017.

Received March 17, 2008
in revised form June 2, 2008